# A Novel ZCS High Frequency Inverter in Complex Resonance Applied for Reduction of PM

Sachio Kubota
Toba National College of Maritime Technology
1-1 Ikegami-cho Toba-shi, Mie 517-8501, Japan
Phone +81-599-25-8005 Fax +81-599-25-8005
E-mail: kubota@toba-cmt.ac.jp

Yoshihiro Hatanaka
Tokyo University of Mercantile Marine
2-1-6 Echujima Koto-ku, Tokyo 135, Japan
Phone +81-3-5245-7407 Fax +81-3-5245-7336
E-mail: hatanaka@ipc.tosho-u.ac.jp

**ABSTRACT**- A novel ZCS high frequency inverter in complex resonance applied for reduction of PM is developed. This inverter is suppressed the switching stress by using complex resonance. The stable operation is realized by ZCS using overlapping commutation phenomenon. The ZCS characteristics are investigated based on numerical analysis and experimental results.

## 1.INTRODUCTION

Recently, the environmental pollution becomes the worldwide problem, and the emission control of the exhaust gas from diesel engine has attracted special interest. The emission control of diesel engine used for the vehicle or the marine engine has been examined variously, because PM( Particulate Matter) in the exhaust gas is noted as one of the factor to cause a lung cancer and an allergy. So, authors have already proposed the system which reduces PM, according to burning it by utilizing high frequency induction heating.[1]

In this paper, the power supply for induction heating is examined in detail. In the past, the high frequency inverters have been used for the power supply of high frequency induction heating. However there are many problems by high frequency operation. As the solution of these problems, various soft switching techniques such as ZCS( Zero Current Switching) and ZVS( Zero Voltage Switching) have been investigated. However, these inverters tend to complicate the composition of circuit, because an auxiliary switch and a circuit for commutation is usually needed for these soft switching operation. Therefore, a novel ZCS high frequency inverter in complex resonance which is realized the suppression of the switching stress by ZCS using complex resonance in spite of simple circuit composition is proposed. Furthermore, the ZCS characteristics of the proposed inverter are examined from both sides of the numerical analysis using a normalized parameter and the experimental results.

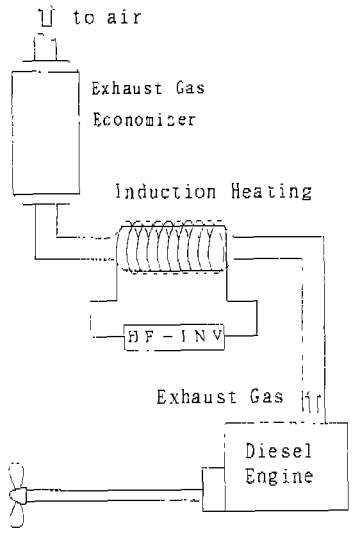


Fig.1 System of emission control

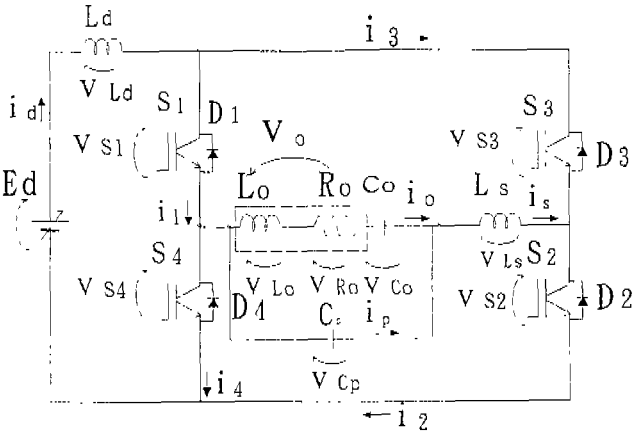


Fig.2 A novel ZCS high frequency inverter in complex resonance

## 2.PM REDUCTION SYSTEM

Fig. 1 shows the outline of the reduction system of PM exhausted from the marine diesel engine. In Fig. 1, PM exhausted from diesel engine is trapped by the metallic

filter inside the induction heating unit connected to the exhaust pipe, and is burned instantly at high temperature when it touched the filter. In this manner, this system reduces PM by the application of high frequency induction heating.

## 3.ZCS HIGH FREQUENCY INVERTER

Fig. 2 shows a novel ZCS high frequency inverter in complex resonance proposed in this paper. The continuity of switching current ( $i1=i2=(id+is)/2$, $i3=i4=(id-is)/2$ ) is established by connection of reactors of Ld and Ls in this circuit. Therefore, the ZCS using the overlapping commutation phenomenon which is led to by continuity of current can be performed.

In this inverter, an input DC reactor is not connected, and the stray inductance of wiring on the input DC branch is used as Ld, because ZCS using overlapping commutation phenomenon is carried out even if Ld is very small. Consequently, the conducting loss and the value of maximum voltage of the switch are suppressed which the size of Ld influences. Moreover, the value of maximum current of the switch is suppressed by using complex resonance which forms a tank circuit, though the load of the induction heating is operated in full load. Therefore, a proposed inverter realizes the ZCS operation by simple circuit composition without auxiliary switches and auxiliary circuits, and suppresses the switching stress.

## 4.PRINCIPLE OF OPERATION

The switching mode of the proposed inverter is classified into seven modes of the following due to the switching condition.

mode(a): S1-S2 single conduction mode
mode(b): D1-D2 single conduction mode
mode(c): D1-D2,S3-S4 double conduction mode
mode(d): S3-S4 single conduction mode
mode(e): D3-D4 single conduction mode
mode(f): D3-D4,S1-S2 double conduction mode
mode(g): OFF mode

Each switching operation mode is illustrated in the Fig. 3.

Fig. 4 illustrates the switching wave forms in ZCS operation on relation to each switching mode and switching state of the switches. The following expression is derived from the symmetry of the circuit in the full bridge inverter by the main circuit composition in Fig. 2.

$$i1=i2=(id+is)/2 \quad \cdots (1)$$

$$i3=i4=(id-is)/2 \quad \cdots (2)$$

*id* is the DC current which flow through the stray

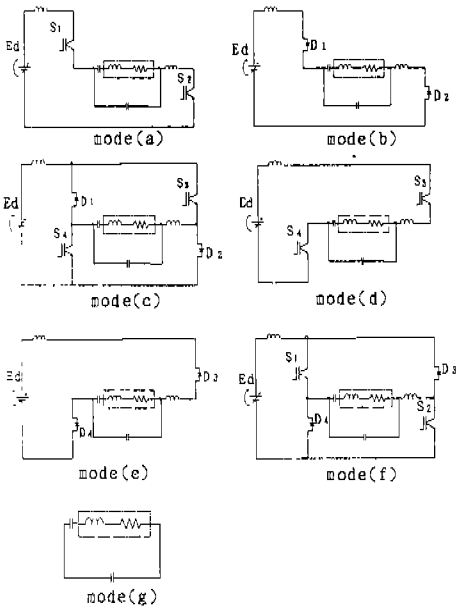


Fig. 3 Switching operation mode

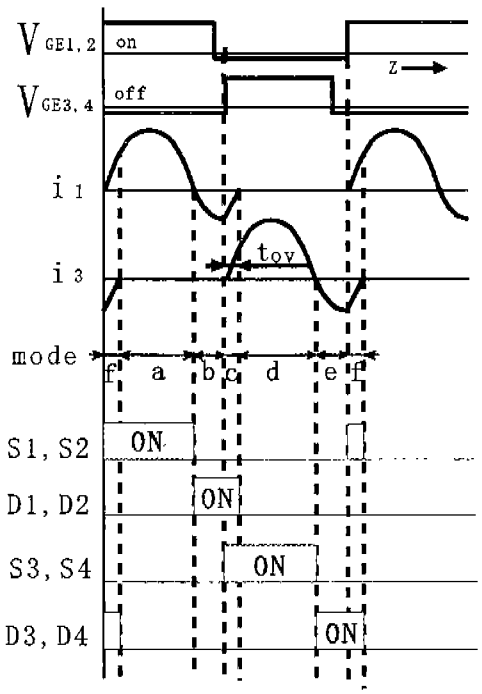


Fig.4 Switching wave form in ZCS operation

inductance of Ld, and *is* is the resonant current which flow through the reactor of Ls. Because these current do not jump instantly, the continuity of these current which flow through each switching element is established. Therefore, the double conduction mode such as mode (c) and mode(f) in Fig. 4 occur. This phenomenon is called as an overlapping commutation. By using overlapping commutation, the ZCS operation of all the switching elements is realized.[2]

## 5.ANALYSIS

The ZCS characteristics have to be grasped in order to drive the high frequency inverter for induction heating under optimum frequency band and load condition. Then, the characteristics of the proposed inverter are analyzed by numerical analysis, and the boundary region between ZCS and non-ZCS is clarified when a operating frequency and load condition are changed. The numerical analysis is carried out using normalized parameter which are shown in Table 1 in order to give the degree of freedom in the circuit design.

The normalized state equations of each switching mode as shown in Fig. 3 are described as follows.

mode(a)

$$\frac{dVcp^*}{dz}=\frac{2\pi}{\mu}\cdot\frac{1}{p}\cdot(is-io)$$
$$\frac{dVco^*}{dz}=\frac{2\pi}{\mu}\cdot io$$
$$\frac{dio^*}{dz}=\frac{2\pi}{\mu}\cdot(Vcp-Vco-\lambda\cdot io)$$
$$\frac{dis^*}{dz}=\frac{2\pi}{\mu}\cdot\frac{1}{\alpha+\beta}\cdot(1+Vcp)$$
$$\frac{did^*}{dz}=\frac{2\pi}{\mu}\cdot\frac{1}{\alpha+\beta}\cdot(1+Vcp)$$

mode(b)

$$\frac{dVcp^*}{dz}=\frac{2\pi}{\mu}\cdot\frac{1}{p}\cdot(is-io)$$
$$\frac{dVco^*}{dz}=\frac{2\pi}{\mu}\cdot io$$
$$\frac{dio^*}{dz}=\frac{2\pi}{\mu}\cdot(Vcp-Vco-\lambda\cdot io)$$
$$\frac{dis^*}{dz}=\frac{2\pi}{\mu}\cdot\frac{1}{\alpha+\beta}\cdot(1+Vcp)$$
$$\frac{did^*}{dz}=\frac{2\pi}{\mu}\cdot\frac{1}{\alpha+\beta}\cdot(1+Vcp)$$

mode(c)

$$\frac{dVcp^*}{dz}=\frac{2\pi}{\mu}\cdot\frac{1}{p}\cdot(is-io)$$
$$\frac{dVco^*}{dz}=\frac{2\pi}{\mu}\cdot io$$
$$\frac{dio^*}{dz}=\frac{2\pi}{\mu}\cdot(Vcp-Vco-\lambda\cdot io)$$
$$\frac{dis^*}{dz}=-\frac{2\pi}{\mu}\cdot\frac{1}{\beta}\cdot Vcp$$
$$\frac{did^*}{dz}=\frac{2\pi}{\mu}\cdot\frac{1}{\alpha}$$

mode(d)

$$\frac{dVcp^*}{dz}=\frac{2\pi}{\mu}\cdot\frac{1}{p}\cdot(is-io)$$
$$\frac{dVco^*}{dz}=\frac{2\pi}{\mu}\cdot io$$
$$\frac{dio^*}{dz}=\frac{2\pi}{\mu}\cdot(Vcp-Vco-\lambda\cdot io)$$
$$\frac{dis^*}{dz}=-\frac{2\pi}{\mu}\cdot\frac{1}{\alpha+\beta}\cdot(1+Vcp)$$
$$\frac{did^*}{dz}=\frac{2\pi}{\mu}\cdot\frac{1}{\alpha+\beta}\cdot(1+Vcp)$$

mode(e)

$$\frac{dVcp^*}{dz}=\frac{2\pi}{\mu}\cdot\frac{1}{p}\cdot(is-io)$$
$$\frac{dVco^*}{dz}=\frac{2\pi}{\mu}\cdot io$$
$$\frac{dio^*}{dz}=\frac{2\pi}{\mu}\cdot(Vcp-Vco-\lambda\cdot io)$$
$$\frac{dis^*}{dz}=-\frac{2\pi}{\mu}\cdot\frac{1}{\alpha+\beta}\cdot(1+Vcp)$$
$$\frac{did^*}{dz}=\frac{2\pi}{\mu}\cdot\frac{1}{\alpha+\beta}\cdot(1+Vcp)$$

mode(f)

$$\frac{dVcp^*}{dz}=\frac{2\pi}{\mu}\cdot\frac{1}{p}\cdot(is-io)$$
$$\frac{dVco^*}{dz}=\frac{2\pi}{\mu}\cdot io$$
$$\frac{dio^*}{dz}=\frac{2\pi}{\mu}\cdot(Vcp-Vco-\lambda\cdot io)$$
$$\frac{dis^*}{dz}=-\frac{2\pi}{\mu}\cdot\frac{1}{\beta}\cdot Vcp$$
$$\frac{did^*}{dz}=\frac{2\pi}{\mu}\cdot\frac{1}{\alpha}$$

Table 1 Normalized Parameters

【Normalized Value】
Frequency $\mu=2\pi fo\sqrt{LC}$ L=Lo
Load Resistance $\lambda=R/\sqrt{L/C}$ C=Co
Reactance $\alpha$ =Ld/L $\beta$ =Ls/L R=Ro
Capacitance p=Cp/C
【Reference Value】
Voltage E=Ed Current $I=E/\sqrt{L/C}$
Power P=EI Impedance $z=\sqrt{L/C}$
Time T=1/fo fo: output frequency
【State Variable】
Voltage $v^*(z)=v(t)/E$
Current $i^*(z)=i(t)/I$
Power Po*=Po/P Time z=t/T=fo · t

Table 2 Comparison of the ZCS characteristics in changing $\beta$

| $\beta$, p | small | ⇔ | large |
|---|---|---|---|
| apparent power factor | × low | | ○ high |
| *Vsmax* | × high | | ○ low |
| *Ismax* | × high | | ○ low |
| ZCS region | ○ wide | | × nallow |

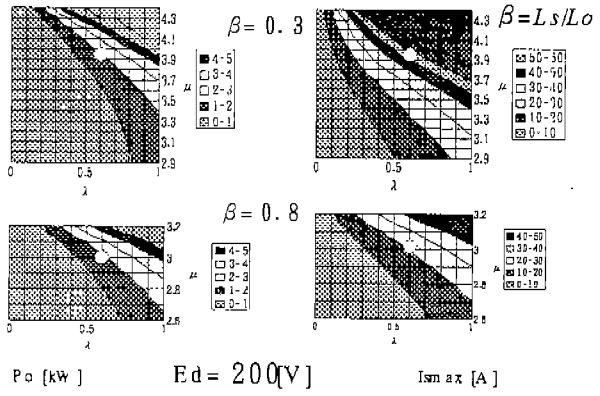


Fig.5 Distribution of Po and Ismax

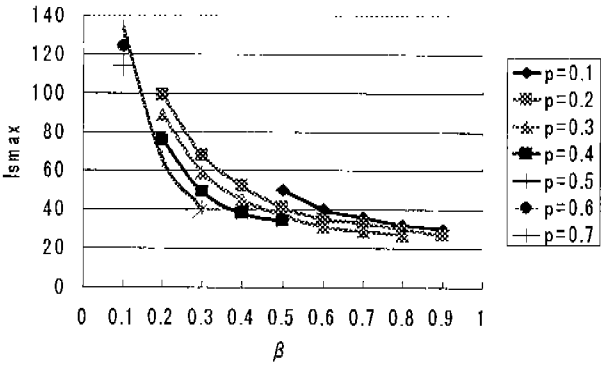


Fig.6 Comparison of Ismax by changing $\beta$

mode(g)

$$\frac{dVcp*}{dz}=-\frac{2\pi}{\mu}\cdot\frac{1}{p}\cdot io$$

$$\frac{dVco*}{dz}=\frac{2\pi}{\mu}\cdot io$$

$$\frac{dio*}{dz}=\frac{2\pi}{\mu}\cdot(Vcp-Vco-\lambda\cdot io)$$

$$\frac{dis*}{dz}=0$$

$$\frac{did*}{dz}=0$$

Each normalized state equation are analyzed by fourth order Runge-Kutta method.

## 6.ZCS CHARACTERISTICS

In the proposed inverter using complex resonance, the circuit parameters, such as reactor ratio of $\alpha$ and $\beta$, capacitance ratio of p, the normalized frequency of $\mu$ and the normalized resistance of $\lambda$, much affect the circuit operation. And this inverter suppresses the switching stress by choices of the optimum parameters. The ZCS operation region and the switching stress are affected by the change of $\alpha$, $\beta$ and p.

As the results of the numerical analysis, Table 2 shows the effect on the ZCS characteristics, such as the ZCS operation region, the maximum voltage of the switch of Vsmax and the maximum current of the switch of Ismax as the switching stress, by change of $\beta$ and p. Vsmax and Ismax are suppressed by enlarging $\beta$ and p, because the power factor is improved. However the ZCS operation region becomes narrow. Then, the distribution of each characteristic value, such as Ismax, Vsmax, Po, real power factor of cos $\phi$ and apparent power factor of cos $\phi$ ', within the ZCS operation region are investigated.

Fig. 5 shows the distribution of the output power of Po [kW] in the ZCS operation region and the maximum value of the current of the switch of Ismax[A] by change of $\beta$ when input DC voltage is 200[V]. Each characteristics are calculated for load resistance of 5 [Ω] and load inductance of 100[$\mu$H] as the constants of the equivalent circuit of the induction heating load. Each characteristics are shown in nomalized $\mu$ - $\lambda$ plane. Here, the change of $\mu$ and $\lambda$ means the change of frequency and capacitor, respectively.

The white point as shown in this figure is 2[kW] of output power when the load parameter of $\lambda$ is designed as $\lambda$ =0.6. From this figures, Ismax at $\beta$ =0.3 shows 65[A] and Ismax at $\beta$ =0.8 shows 21[A]. Ismax at $\beta$ =0.8 can be suppressed more than Ismax at $\beta$ =0.3 although the ZCS operation region at $\beta$ = 0.3 is larger than the ZCS operation region at $\beta$ = 0.8.

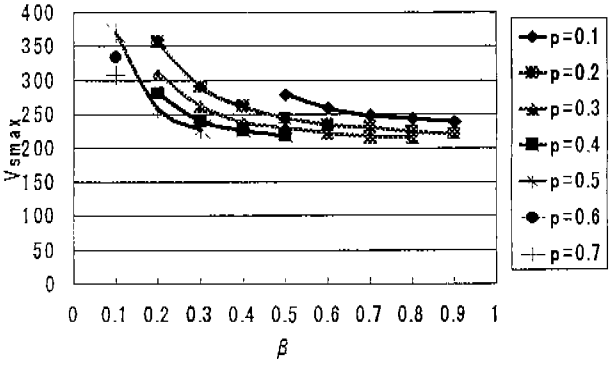


Fig.7 Comparison of Vsmax by changing $\beta$

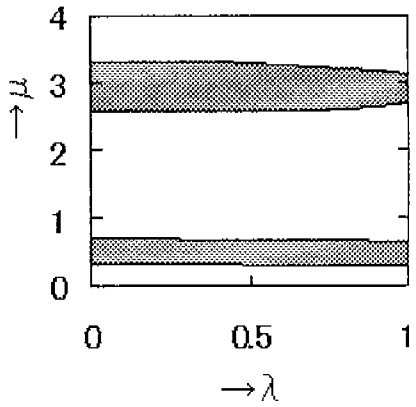


Fig. 8 ZCS operation region

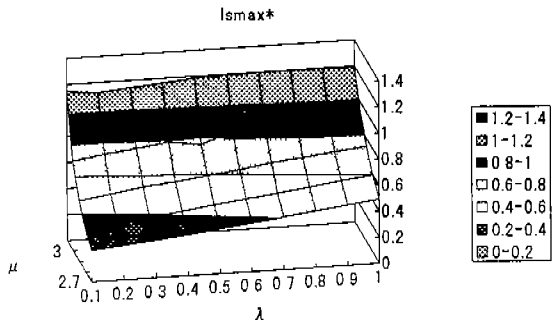


Fig. 9 Distribution of Ismax*

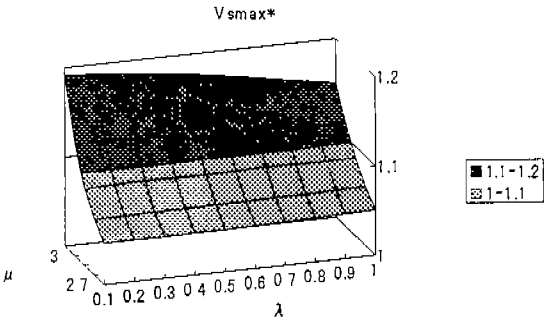


Fig. 10 Distribution of Vsmax*

In the same way as Fig. 5, the influences to Ismax and Vsmax by change of $\beta$ and p are shown in Fig. 6 and Fig. 7 respectively when $\lambda$ is designed as $\lambda$ =0.8. The point is not written in this figure, when the ZCS operation is not performed or output power is under 2 [kW].

From these figures, Ismax and Vsmax as the switching stress is suppressed by enlarging $\beta$ and p. And Vsmax is approximately equal to the power supply voltage when $\beta$ is larger than 0.3. However it is much higher than the power supply voltage when $\beta$ is smaller than 0.3.

In this inverter, Ld is very small because the inductance of wiring is used for. Therefore, $\alpha$ is designed as $\alpha$ =0.05 and is suppressed Vsmax to low as a result.

However, the region where p is larger than 0.8 or $\beta$ is larger than 1 becomes non-ZCS operation region, because the ZCS operation region narrows by enlarging $\beta$ and p. Therefore, when the circuit is designed, it is important to choice the optimum parameters in order to suppress the switching stress and maintain a wide ZCS operation region.

When the parameters of $\beta$ =0.8 and p=0.3 are chosen, the switching stress can be suppressed to the lowest. However the drive of the inverter becomes severe because the ZCS operation region is narrow. As for the circuit parameters, $\beta$ =0.8 and p=0.2 are chosen from the above consideration.

Fig. 8 shows the ZCS operation region on the normalized $\mu$ - $\lambda$ plane in $\beta$ =0.8 and p=0.2. As for this circuit, the ZCS operation region appears on two frequency bands by using the complex resonance. Thereby the double frequency induction heating is possible by one inverter. This time, in order to drive at one frequency band, the high part of $\mu$ which is wide ZCS operation region is investigated and is used.

Fig. 9 shows the distribution of the normalized maximum voltage of the switch of Vsmax* in the ZCS operation region on the normalized $\mu$ - $\lambda$ plane. Vsmax* in the ZCS operation region is suppressed to less than 1.2 times of Ed of the power supply voltage, and in the region of low $\mu$ , is almost equal to Ed.

Fig. 10 shows the distribution of the normalized maximum current of Ismax* as well as Fig. 9.

Both Vsmax* and Ismax* is not influenced by change of $\lambda$ , and is influenced by change of $\mu$ . Moreover, both characteristic values can be suppressed to low in the region of low $\mu$ .

Similarly, Fig. 11 shows the distribution of Po *. In this figure, Po* becomes high by enlarging $\mu$ and $\lambda$ . From consideration from Fig. 9 to Fig. 11, the region where high power is obtained with suppressing the switching stress is the region of low $\mu$ and large $\lambda$ .

Fig. 12 and Fig. 13 show the distribution of apparent power factor of cos $\phi$ ' in the part of Lo-Ro and distribution of real power factor of cos $\phi$ in the tank circuit respectively within the ZCS operation region.

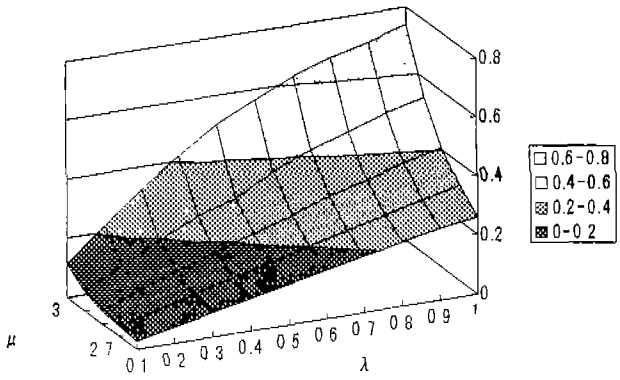


Fig. 11 Distribution of Po*

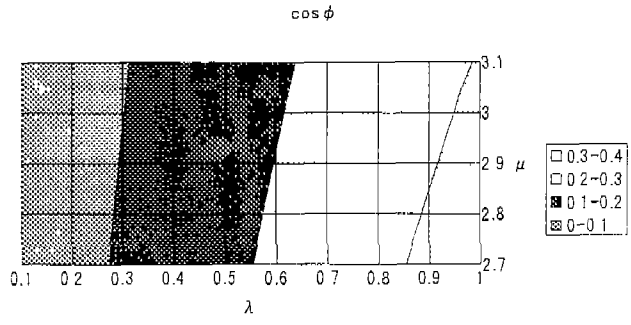


Fig. 12 Distribution of real power factor

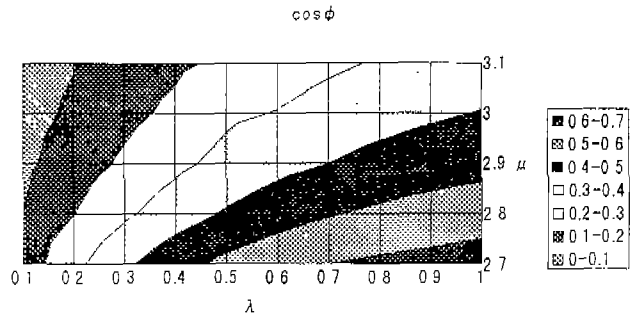


Fig. 13 Distribution of apparent power factor

Table 3 Specification of power supply

| |
|---|
| Output power: 1.2 [ kW ] |
| Input voltage: 0 ~ 300 [ V ] |
| Heating temperature: 273 ~ 890 [ K ] |
| Output frequency : 22 [ kHz ] |
| Normalized parameters : |
| $\mu$ =2.7, $\lambda$ =0.6, $\alpha$ =0.05, $\beta$ =0.8, p=0.2 |
| Circuit constants : |
| Ro=3.5 ~ 5 [ Ω ] Lo=100 [ $\mu$ H ] |
| Ls=80 [ $\mu$ H ] |
| Co=4.0 [ $\mu$ F ] Cp=0.8 [ $\mu$ F ] |
| Device |
| IGBT :2MBI50J-060 (600V/50A) |

Apparent power factor is improved in comparison with real power factor. Consequently, as the switching stress is suppressed, high power can be obtained. And, the point of low $\mu$ and large $\lambda$ within ZCS operation region in Fig. 13 is suitable as the driving point, because the switching stress is suppressed by high power factor. This result agrees with the above-mentioned result from Fig. 9 to Fig. 11. However, the resistance of induction heating load is so small that $\lambda$ has a limit in enlarging.

From these general considerations, the normalized parameters of $\lambda$ =0.6 and $\mu$ =2.7 are chosen for circuit design.

## 7.EXPERIMENTAL RESULTS

The power supply in induction heating system for reduction of PM has been designed on the basis of the results by numerical analysis, and fundamental experiment of combustion of PM has been carried out. Table 3 shows the specification of power supply.

The appearance of the induction heating unit for reduction of PM is shown in Fig. 14. This induction heating unit is composed of the working coil for induction heating and the metallic filter to trap PM.

Fig. 15 shows the state of combustion of PM. PM is burned instantly when it touched the metallic filter, because the filter is heated in the high temperature more than 850[K]. In this manner, the reduction of PM is realized.

Fig. 16 shows the comparison of the theoretical wave form based on the numerical analysis and the experimental wave form using the high frequency induction heating load. In Fig. 16, similarity between theoretical results and experimental results is verified. Consequently, the correctness of the theory is proved.

And the stable operation suppressing the spike voltage and surge current is realized by ZCS using overlapping commutation phenomenon. Furthermore by composition of a tank circuit, great amplitude operation of output current of *io* is realized, though the maximum value of *il* of the current of switch is suppressed.

## 8.CONCLUSION

In this paper, we proposed a novel ZCS high frequency inverter in complex resonance applied for reduction of PM. Though the composition of circuit is simple, the realization of the stable operation by ZCS using overlapping commutation phenomenon is proved through the experiment of combustion of PM.

And switching stress is suppressed by choosing the optimum parameter in complex resonance

In the near future, we would like to prove that PM reduction by driving a real marine diesel engine.

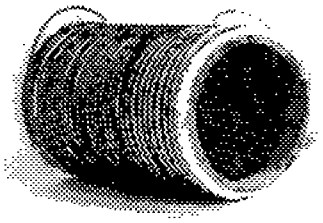

Fig.14 Induction heating unit

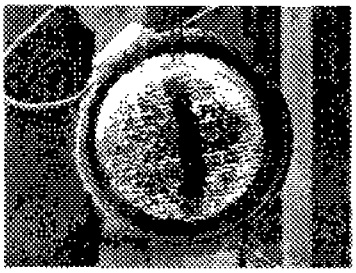

Fig.15 Combustion of PM

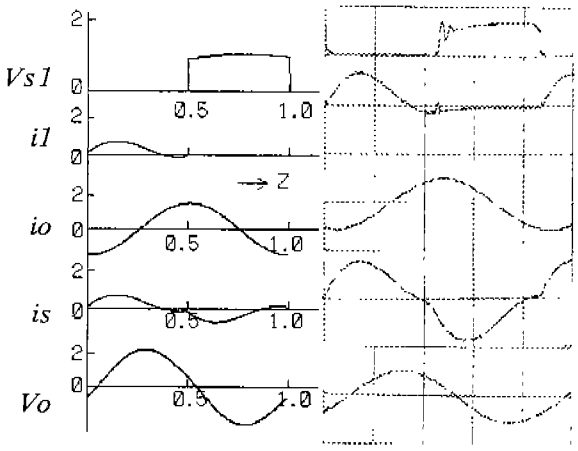


Numerical analysis Experiment

10 $\mu$ s/div,200V/div(Vs1),20A/div(i1),
50A/div(io),20A/div(is),500V/div(Vo)

Fig. 16 Comparison of wave forms

## 9.REFERENCES

[1]Y.Hatanaka, S.Kubota and Y.Sekiya, "Novel zero current switching high frequency inverter applied for an emission control in diesel engine," in Proceeding of EPE'97,1997

[2]S.Kubota, Y.Hatanaka, "A Novel High Frequency Power Supply for Induction Heating," in Proceeding of PESC'98 Vol.1 pp.165-171,1998

[3]S.Kubota, Y. Hatanaka, "ZCS High Frequency Inverter for Induction Heating in Complex Resonance," in Proceeding of National Convention of I.E.E.Japan, pp.4.239,1998